Optimal Segregation of Proteins: Phase Transitions and Symmetry Breaking

Jie Lin, Jiseon Min, and Ariel Amir

Phys. Rev. Lett. **122**, 068101 — Published 13 February 2019

DOI: 10.1103/PhysRevLett.122.068101

Optimal segregation of proteins: phase transitions and symmetry breaking

Jie Lin,[1] Jiseon Min,[1,2] and Ariel Amir[1]

[1] *School of Engineering and Applied Sciences, Harvard University, Cambridge, Massachusetts 02138, USA*
[2] *Department of Physics, California Institute of Technology, Pasadena, California 91125, USA*

(Dated: January 18, 2019)

Asymmetric segregation of key proteins at cell division – be it a beneficial or deleterious protein – is ubiquitous in unicellular organisms and often considered as an evolved trait to increase fitness in a stressed environment. Here, we provide a general framework to describe the evolutionary origin of this asymmetric segregation. We compute the population fitness as a function of the protein segregation asymmetry a, and show that the value of a which optimizes the population growth manifests a phase transition between symmetric and asymmetric partitioning phases. Surprisingly, the nature of phase transition is different for the case of beneficial proteins as opposed to deleterious proteins: a smooth (second order) transition from purely symmetric to asymmetric segregation is found in the former, while a sharp transition occurs in the latter. Our study elucidates the optimization problem faced by evolution in the context of protein segregation, and motivates further investigation of asymmetric protein segregation in biological systems.

Introduction - In stressed environments, microbial cells such as bacteria or yeast utilize various mechanisms in order to survive. One important mechanism is the asymmetric segregation of vital cytosolic components at cell division: one of the two daughter cells will inherit more favorable conditions (at the expense of the sister cell) [1–6]. Experiments on fission yeast have shown that this asymmetric segregation emerges only in a stressed environment [7]. These observations led to a conjecture that cells may have evolved asymmetric segregation of deleterious damages to increase the overall fitness of the population since one of the daughter cells would be "rejuvenated" [3, 8–10]. Cytosolic components that are advantageous to cell growth may also be segregated asymmetrically [11, 12]. For instance, recent experiments elucidated the molecular mechanisms of asymmetric segregation of the main multidrug efflux pumps in the bacterium *Escherichia coli*, which enable direct expulsion of harmful chemicals from the cells [12]. The strong partitioning bias of efflux pumps for the old cell poles generates growth rate differences among cells, and it has been argued to be a strategy for bacteria to survive a high concentration of antibiotics.

Several previous theoretical works focused on particular models for how damage affects cellular growth, in which it was shown that completely asymmetric segregation (one daughter cell inherits all the key protein from the mother cell) optimizes the population growth rate [3, 9, 13]. Here, rather than focusing on a particular model, we will study a rather broad class of models in which the instantaneous (single-cell) growth rate is a function of the protein concentration. Notably, we will find the optimal segregation strategy that maximizes the population growth rate [14, 15]. In this way, we obtain general insights into the problem and identify the underlying optimization principles. Also, previous studies often consider a coarse-grained effect of the damaged proteins on the cell's fitness through the generation time [3, 13] or the survival rate [9], neglecting the exponential growth of cell volume at the single level [16–19]. A more realistic model should start from the instantaneous effects of the key protein cellular concentration on the single-cell growth rate.

For the completely asymmetric segregation case, we derive an analytical expression for the population growth rate. For weak asymmetry, we can map the problem to the Landau theory of phase transitions [20]. We find that the optimal ratio exhibits a phase transition from a symmetric phase to a perfectly asymmetric phase as the environmental stress increases. While the transition is sharp for the case of deleterious proteins, for the segregation of benefits the transition is of second order. These theoretical predictions are verified using numerical simulations. We conclude by discussing the relation between our theory and experimental observations.

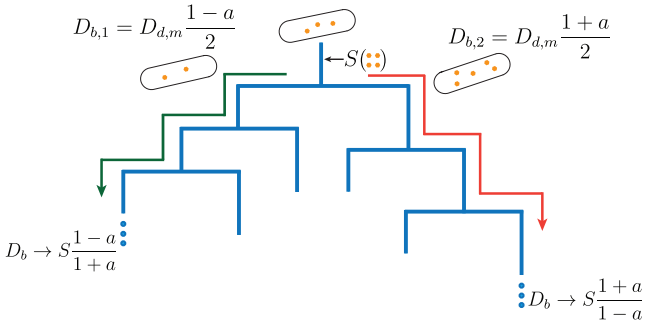

FIG. 1. A mother cell attributes the protein asymmetrically to the daughters, with an asymmetry parameter a. The lineage composed of cells inheriting more proteins than its sister cell will reach a steady state with a constant number of proteins at cell birth (red arrow). Similarly, the other lineage composed of cells inheriting less proteins (green arrow) will reach a steady state.

Model- We assume that the amount of the newly produced key protein is proportional to the increment of cell

volume, with an accumulation rate S. Therefore, the amount of protein at cell volume V is equal to

$$D(V) = D_b + S(V - V_b), \tag{1}$$

and here V_b (D_b) is the cell volume (amount of protein) at cell birth. The protein accumulation rate S quantifies the environmental stress: a larger S represents a more stressed environment for damage segregation, *e.g.*, a higher temperature [7] and a less stressed environment for benefit segregation. In the case of beneficial proteins, the usual parameter tuned in experiments is the concentration of antibiotics [12]. A higher concentration of antibiotics requires a higher concentration of beneficial proteins, *e.g.*, the efflux pump, to achieve the same growth rate as a lower concentration of antibiotics. So increasing the environmental stress through antibiotics concentration is equivalent to lowering the beneficial protein concentrations, which is set by the protein accumulation rate. In the following, we consider the protein accumulation rate as the control parameter for both damage and benefit segregation cases, and a larger (smaller) S represents a more stressed environment for damage (benefit) segregation.

We assume that the cell divides its volume symmetrically and deterministically ($V_b = 1, V_d = 2$) based on the fact that the cell volume fluctuation is small [17, 18, 21, 22]. The amounts of protein that the two daughter cells inherit are

$$D_{b,1} = D_{d,m}\frac{1-a}{2}, \quad D_{b,2} = D_{d,m}\frac{1+a}{2}, \tag{2}$$

where $D_{d,m}$ is the amount of protein inside the mother cell at division, and a is a continuous variable, ranging from 0 to 1 (Fig. 1). $a = 1$ corresponds to the completely asymmetric segregation and $a = 0$ corresponds to the symmetric segregation.

We assume that the cell volume grows exponentially at the single cell level [16, 17, 19],

$$\frac{dV}{dt} = \lambda[\sigma]V, \tag{3}$$

where $\lambda[\sigma]$ is the instantaneous growth rate, depending on the protein concentration $\sigma = D/V$. The growth rate function depends on the specific system, which can be measured experimentally and in general exhibits an inflection point [2, 3]. Here, we consider the growth rate as a Hill-type function,

$$\lambda[\sigma] = \frac{\lambda_0 + \lambda_1\sigma^n}{1+\sigma^n}. \tag{4}$$

If $\lambda_0 > \lambda_1$, $\lambda[\sigma]$ is a decreasing function, and thus the key protein is deleterious. If $\lambda_0 < \lambda_1$, the protein is beneficial. We note that an intrinsic concentration scale K_m is implicitly included in Eq. (4) and set as the unit of concentration. In the following, we set the accumulation rate of the key protein to be $0 < S < 1$ since for all cases we study the phase transition occurs within this range. This is consistent with experimental observations within the framework of our model [2, 3, 7, 12].

In this paper, we focus on the case $n = 2$, but our main conclusions are valid for any $n > 1$ (Supplementary Information [23] (SI) (c)). First, we briefly discuss the special case $n = 1$, where the growth rate function is purely convex (concave) for the damage (benefit) case. In this case, we find that the population growth rate is always maximized at $a = 1$ ($a = 0$) for the damage (benefit) case, independent of the environmental stress (see proofs and numerical tests in SI (b)). This is consistent with the previous work on related models [3, 9].

In the following, we provide two methods to find the population growth rate respectively for small a and $a = 1$, for a general growth rate function with an inflection point. Interpolating between these two limits will provide insights into the optimal degree of asymmetry.

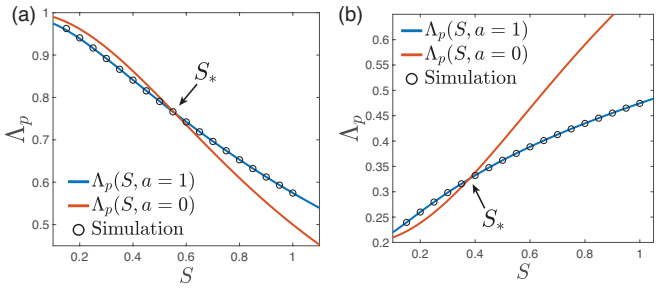

FIG. 2. The population growth rate at $a = 0$ and $a = 1$ for the damage (a) and benefit (b) case. The blue solid lines are theoretical results based on numerical calculation of Eq. (5), and the red solid lines are $\lambda[S]$. The circles are results from direct simulations of a population with $a = 1$. S_* is the accumulation rate at which $\Lambda_p(S_*, 0) = \Lambda_p(S_*, 1)$. The growth rate at the single-cell level is equal to $\lambda[\sigma] = \frac{\lambda_0+\lambda_1\sigma^2}{1+\sigma^2}$ with $\lambda_0 = 1$, $\lambda_1 = 0$ for the damage case and $\lambda_0 = 0.2$, $\lambda_1 = 1.2$ for the benefit case. Note that $\lambda_0 > 0$ for the benefit case in order to ensure a well defined population growth rate also for perfectly asymmetric partitioning. The value of λ_0 does not affect our conclusions (see SI (f)). $S_* \approx 0.558$ for the damage case and $S_* = 0.378$ for the benefit case.

Self-similarity method - We consider an exponentially growing population and imagine taking a snapshot of the population at some time, from which we can find the total number of cells (N) and the total cell volume of the whole population (V_t). The population growth rate must be equal to the total volume growth rate $\frac{1}{N}\frac{dN}{dt} = \frac{1}{V_t}\frac{dV_t}{dt} = \Lambda_p$ because the cell volume is regulated. We use the total cell volume to compute Λ_p because it is more accurate and tractable to measure the growth rate of the total cell volume than total cell number in numerical simulations and analytical analysis.

When $a = 0$, the concentration of the key protein remains constant as the cell is growing from $V = 1$ to

$V = 2$, and is equal to the accumulation rate, S, of the key protein. Therefore, all cells grow at the same rate $\lambda[S]$, and the population growth rate is equal to the homogeneous single-cell growth rate $\Lambda_p = \lambda[S]$.

When $a = 1$, one of the daughter cells does not get any of the key protein from its mother, while the other one inherits all the key protein. This leads to a self-similarity in the population tree (see the illustration in Fig. A1 in the SI). Consider a tree starting from a single cell without any key protein. The whole tree can then be decomposed into subtrees, which are identical to the original one, except for a temporal shift. The number of cells of the whole tree grows as $N(t) \sim \exp(\Lambda_p t)$. The subtrees share the same Λ_p as the whole tree, but with a temporal shift, $\sum_{j=0}^{i} \tau_j(S))$ $(i = 0, 1, 2, ...)$, where $\tau_j(S)$ is the generation time of a cell whose amount of key protein at cell birth is jS (SI (d)). The self-consistent equation of the population growth rate is

$$\sum_{i=0}^{\infty} \exp\Big(- \Lambda_p \sum_{j=0}^{i} \tau_j \Big) = 1. \tag{5}$$

The above equations are satisfied by a unique value of population growth rate Λ_p. In Fig. 2(a,b), we plot the numerical values of Λ_p when $a = 1$ based on Eq. 5. We note that both for the damage and benefit cases, there exists a special S_* at which $\Lambda_p(S_*, a = 1) = \Lambda_p(S_*, a = 0) = \lambda[S_*]$. For the damage (benefit) case, $a = 0$ is favored to $a = 1$ if $S < S_*$ $(S > S_*)$, and $a = 1$ is favored to $a = 0$ if $S > S_*$ $(S < S_*)$ (Fig. 2(a,b)). Yet, comparing the two exactly solvable cases ($a = 0$ and $a = 1$) is not sufficient for finding the optimal a_c which maximizes the population growth rate. Moreover, this comparison does not show how a_c changes with the control parameter S. In the following section, we will introduce the Landau approach and show that S_*, with the inflection point S_c of the growth rate function, determines the nature of the transition from $a_c = 0$ to $a_c = 1$.

Landau approach - We next consider the general case with $a \neq 0$. We decompose the growth of total cell volume (V_t) as the sum of all individual cell contributions, $dV_t/dt = \sum_i \lambda[\sigma_i] V_i$. Because when $a = 0$, all cells have the same protein concentration S, we choose to expand around $\sigma_i = S$ for each cell,

$$\frac{dV}{dt} = \sum_i \lambda[\sigma_i] V_i = V\lambda[S] + \sum_i \frac{d\lambda}{d\sigma}\Big|_S (\sigma_i - S) V_i + \frac{1}{2}\frac{d^2\lambda}{d\sigma^2}\Big|_S (\sigma_i - S)^2 V_i + ...$$

The first order term vanishes because the total amount of protein of the entire population, $\sum \sigma_i V_i = S V_t$ in the steady state. We define the population's fitness as $f = \Lambda_p - \lambda[S]$,

$$f(S, a) = \frac{1}{2}\frac{d^2\lambda}{d\sigma^2}\Big|_S \langle (\sigma_i - S)^2 \rangle_v + ...$$

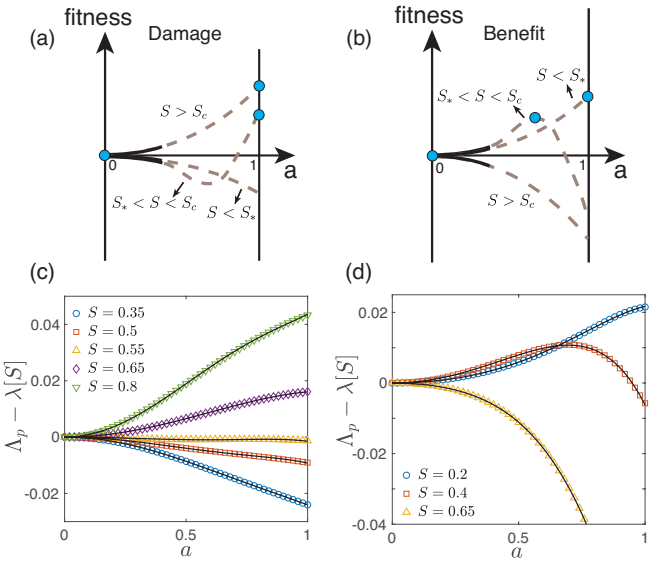

FIG. 3. (a) For the damage case, if $S_* < S_c$, the fitness at $a = 1$ will flip its sign from negative to positive before its curvature at $a = 0$ flip its sign from negative to positive as S increases from 0. This leads to a first order transition of the optimal asymmetry parameter a_c from 0 to 1. The transition of a_c should be sharp as well if $S_* \approx S_c$, because the fitness at $a = 1$ and its curvature at $a = 0$ flip their signs simultaneously. (b) For the benefit case, because S_* is far below S_c, as one increases S from a low value, a small finite a must exist that maximizes the fitness if S is just below S_c This leads to a smooth second order transition with a mean field exponent, $a_c \sim (S_c - S)^{1/2}$. In (a,b), the optimal a_c that maximizes the fitness for different S is labeled by the blue circle. (c,d) Numerical simulations of the fitness as function of a for the damage (c) and benefit (d) cases. Note that in (c), $S_* \approx S_c$, implying that the intermediate regime where the fitness is non-monotonic (as illustrated in part (a) of the figure) is very narrow. For an example of this intermediate scenario see Fig. S5(f). The black lines are the fits based on $f = C_2 a^2 + C_4 a^4 + C_6 a^6$.

where $\langle (\sigma_i - S)^n \rangle_v \equiv (\sum_i (\sigma_i - S)^n V_i) / \sum_i V_i$. Note that the fitness is directly related to the variability of protein concentration arising from the deterministic asymmetric partitioning, thus contributing to the population's phenotypic heterogeneity. In the symmetric case ($a = 0$), the fitness f is zero by definition. Consider now the limit $0 < a \ll 1$. Because in the limit of small a, $\langle (\sigma_i - S)^n \rangle_v \sim a^n$, the lowest order term of the fitness function has to scale as a^2 with its coefficient proportional to the second derivative of the growth rate function at S,

$$f = AS^2 \frac{d^2\lambda}{d\sigma^2}\Big|_S a^2 + C_4(S) a^4 + C_6(S) a^6 + O(a^8). \tag{6}$$

Here A is a universal positive number independent of the growth rate function (SI (h)). The odd order terms vanish because of the symmetry $f(a) = f(-a)$, and C_4, C_6 are constants given a fixed S. We therefore see that the

sign of the second derivative of the growth rate function determines whether the symmetric phase $a = 0$ is a local maximum or minimum of the fitness. The inflection point S_c of the growth rate function, at which its second derivative vanishes, will be central to the analysis.

For the damage case, we find $S_* \approx S_c$ ($S_* = 0.558$, $S_c = 0.577$, Fig. 2(a)) taking $\lambda_0 = 1$, $\lambda_1 = 0$. We numerically confirm this is true for other Hill exponents n (SI (c)) and prove $S_* \approx S_c$ if $\lambda_1 = 0$ (SI (d)). As one increases the protein accumulation rate, the fitness at $a = 1$ changes from negative to positive when S exceeds S_*, and the curvature of the fitness at $a = 0$ changes from negative to positive when S exceeds S_c (Fig. 3(a)). Therefore, if $S_* < S_c$, as one increases S, the fitness at $a = 1$ changes from negative to positive before the curvature at $a = 0$ changes its sign. Assuming a smooth interpolation of the fitness function from $a = 0$ to $a = 1$, a_c should undergo a first order transition from 0 to 1 as S increases (Fig. 3(a)). In particular, the transition of a_c should be sharp as well if $S_* \approx S_c$, because the fitness at $a = 1$ and its curvature at $a = 0$ flip their signs simultaneously. In SI (f), we also numerically confirm $S_* < S_c$ for a finite λ_1, so a sharp transition is generally true for a Hill function which decreases monotonically. We remark that in the case $S_* < S_c$, the fitness can exhibit a minimum at a finite smaller than with the maximum at $a = 1$. This non-monotonic shape of fitness can affect the accessibility of the fitness maximum during the course of evolution (Fig. S5(f)). In other words, it is insufficient in this case for cells to develop a mild asymmetry of segregation that will evolve slowly towards larger value: the evolutionary advantage presents itself only at a critical value of asymmetry, namely Δa.

For the benefit case, we find $S_* < S_c$ ($S_* = 0.378$, $S_c = 0.577$, Fig. 2(b)) with $\lambda_0 = 0.2$, $\lambda_1 = 1.2$. We numerically confirm that $S_* < S_c$ for other choices of Hill exponent (SI (c)) and λ_0 (SI (f)). We also rigorously prove $S_* < S_c$ in the limit $\lambda_0 \to 0$ (SI (d)). As one increases S from a low value, the fitness at $a = 1$ changes from positive to negative when S exceeds S_* and the curvature at $a = 0$ changes from positive to negative when S exceeds S_c (Fig. 3(b)). Therefore, if $S_* < S_c$, a small finite a must exist that maximizes the fitness if S is just below S_c, and thus we predict a smooth transition of the optimal a_c (Fig. 3(b)). Moreover, by finding the optimal a_c that maximize the fitness using Eq. (6), we predict that the smooth transition of the benefit case is in the universality of the Landau mean field model, namely, $a_c \sim |S - S_c|^{1/2}$ [20]. Our conclusion regarding the sharp transition of a_c for the damage case and the smooth transition for the benefit case is generally true for different types of growth rate function (SI (i)). In SI(e), we also explain how to intuitively understand why the relations between S_* and S_c are different in the damage and benefit cases. The main idea is to consider a large Hill exponent n and estimate the population growth rate as the average growth rate over all cells in a population. As quantified in the SI, although the growth rate dependence on protein levels in the benefits and damage case has a mirror symmetry, the implications for the population structure are very different.

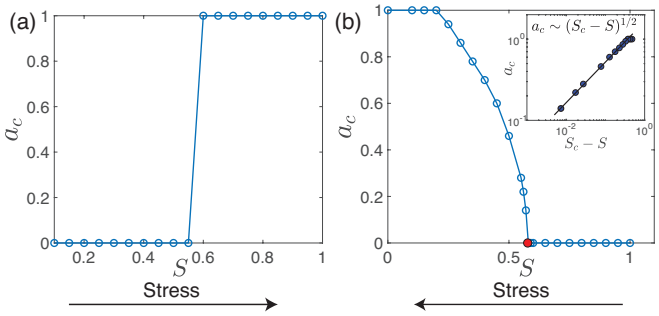

FIG. 4. (a) The optimal a_c changes sharply from 0 to 1 at S_* for the damage segregation. (b) For benefit segregation, the optimal a_c changes smoothly from 1 to 0, vanishing at the critical accumulation rate S_c, the inflection point of the growth rate function (marked as the red circle). The inset shows the mean field scaling near the critical point where the black line has a slope 1/2. Arrows indicate the direction of increasing environmental stress.

Numerical simulations - We test our predictions by simulating an exponentially growing population based on Eqs. (1-4) and by setting $(n, \lambda_0, \lambda_1) = (2, 1, 0)$ for the damage case and $(n, \lambda_0, \lambda_1) = (2, 0.2, 1.2)$ for the benefit case (see simulation details in SI(a)). We compute the fitness as $f = \Lambda_p - \lambda[S]$ and plot it against a in Fig. 3(c,d), which are consistent with Fig. 3(a,b). The optimal a_c that maximizes the fitness changes from $a_c = 0$ to $a_c = 1$ abruptly for the damage case and smoothly for the benefit case, agreeing with our predictions (Fig. 4(a,b)). For the benefit case, the transition shows a second order mean field behavior as we predict (see inset of Fig. 4(b)). Furthermore, we test our Landau approach by fitting the fitness using $f = C_2 a^2 + C_4 a^4 + C_6 a^6$ (black lines in Fig. 3(c,d)). The measured a_c is consistent with the values of a_c inferred from the Landau expansion. We also plot the fit using the first two terms in the Landau expansion which leads to deviations for large a values (SI(g)). In both of the damage and benefit cases, we obtain the coefficient $A \approx 0.361$ (SI (g)). In SI (h), we find that the value of A is independent of the growth rate function, and it equals $1/(4\ln(2)) \approx 0.361$. This is related to the variance of the key protein numbers at cell birth.

Discussion - In this paper we studied the optimal segregation strategy of a protein whose presence may be beneficial or deleterious to cellular growth. We found that the optimal degree of asymmetry which maximizes the population growth rate shows a rich behavior and in particular a phase transition taking a different form in the case of damage or benefit segregation: a sharp transition from purely symmetric to asymmetric segregation is

found in the former, while a smooth (second order) transition from asymmetric to symmetric segregation occurs in the latter. Our results are consistent with the segregation of damaged proteins in certain organisms, such as fission yeast in which a transition from symmetric segregation to asymmetric phase is observed as the environmental stress increases [7, 24–27]. In these organisms, complex molecular machinery, *e.g.*, Hsp16, has evolved that actively fuse damaged proteins to achieve completely asymmetrical segregation between the two daughter cells ($a = 1$). This suggests that cells may have some control over the segregation ratio by tuning the activity levels of the machinery involved in the asymmetric segregation of damaged protein, making the question we studied here relevant to understanding the optimization problem faced by evolution. Similarly, the beneficial drug pumps in *E. coli* are segregated asymmetrically between the old-pole and new-pole daughter cells [12]. Consistent with our predictions, a continuous change of the asymmetry degree a from 0.06 to 0.2 measured from the relative difference between two daughter cells was observed as the subinhibitory antibiotic concentration increases in the experiments.

Our model can be modified to explain asymmetry in various contexts of cell biology. For example, in some organisms, it might be more accurate to consider a as a function of the current state [3, 4]. It would be interesting to investigate the optimal segregation strategy in such a case, where the segregation process is passively controlled by the current protein concentration.

We thank Yohai Bar-Sinai, Miguel Coelho, Michael Moshe, and Andrew Murray for useful discussions. AA thanks the A.P. Sloan foundation, the Milton Fund, the Volkswagen Foundation and Harvard Dean's Competitive Fund for Promising Scholarship for their support. JL was supported by the George F. Carrier fellowship and the National Science Foundation through the Harvard Materials Research Science and Engineering Center (DMR-1420570). JM was funded by Monticello Foundation Internship and the Robert and Delpha Noland Summer Internships.

[1] E. J. Stewart, R. Madden, G. Paul, and F. Taddei, PLoS Biol **3**, e45 (2005).
[2] A. B. Lindner, R. Madden, A. Demarez, E. J. Stewart, and F. Taddei, Proceedings of the National Academy of Sciences **105**, 3076 (2008).
[3] S. Vedel, H. Nunns, A. Košmrlj, S. Semsey, and A. Trusina, Cell Systems **3**, 187 (2016).
[4] M. Coelho, S. J. Lade, S. Alberti, T. Gross, and I. M. Tolić, PLoS Biology **12**, e1001886 (2014).
[5] J. Vaubourgeix, G. Lin, N. Dhar, N. Chenouard, X. Jiang, H. Botella, T. Lupoli, O. Mariani, G. Yang, O. Ouerfelli, *et al.*, Cell Host & Microbe **17**, 178 (2015).
[6] J. Saarikangas, F. Caudron, R. Prasad, D. F. Moreno, A. Bolognesi, M. Aldea, and Y. Barral, Current Biology **27**, 773 (2017).
[7] M. Coelho, A. Dereli, A. Haese, S. Kühn, L. Malinovska, M. E. DeSantis, J. Shorter, S. Alberti, T. Gross, and I. M. Tolić-Nørrelykke, Current Biology **23**, 1844 (2013).
[8] M. Watve, S. Parab, P. Jogdand, and S. Keni, Proceedings of the National Academy of Sciences **103**, 14831 (2006).
[9] M. Ackermann, L. Chao, C. T. Bergstrom, and M. Doebeli, Aging Cell **6**, 235 (2007).
[10] L. Chao, C. U. Rang, A. M. Proenca, and J. U. Chao, PLoS Computational Biology **12**, e1004700 (2016).
[11] N. Avraham, I. Soifer, M. Carmi, and N. Barkai, Molecular systems biology **9**, 656 (2013).
[12] T. Bergmiller, A. M. Andersson, K. Tomasek, E. Balleza, D. J. Kiviet, R. Hauschild, G. Tkačik, and C. C. Guet, Science **356**, 311 (2017).
[13] L. Chao, PLoS Genetics **6**, e1001076 (2010).
[14] E. Powell, Microbiology **15**, 492 (1956).
[15] J. Lin and A. Amir, Cell Systems **5**, 358 (2017).
[16] P. Wang, L. Robert, J. Pelletier, W. L. Dang, F. Taddei, A. Wright, and S. Jun, Current Biology **20**, 1099 (2010).
[17] M. Campos, I. V. Surovtsev, S. Kato, A. Paintdakhi, B. Beltran, S. E. Ebmeier, and C. Jacobs-Wagner, Cell **159**, 1433 (2014).
[18] S. Taheri-Araghi, S. Bradde, J. T. Sauls, N. S. Hill, P. A. Levin, J. Paulsson, M. Vergassola, and S. Jun, Current Biology **25**, 385 (2015).
[19] N. Cermak, S. Olcum, F. F. Delgado, S. C. Wasserman, K. R. Payer, M. A Murakami, S. M. Knudsen, R. J. Kimmerling, M. M. Stevens, Y. Kikuchi, A. Sandikci, M. Ogawa, V. Agache, F. Baleras, D. M. Weinstock, and S. R. Manalis, Nature Biotechnology **34**, 1052 (2016).
[20] P. M. Chaikin and T. C. Lubensky, *Principles of Condensed Matter Physics* (Cambridge university press, 2000).
[21] A. Amir, Phys. Rev. Lett. **112**, 208102 (2014).
[22] P.-Y. Ho, J. Lin, and A. Amir, Annual Review of Biophysics **47**, 251 (2018).
[23] See Supplemental Material at [URL will be inserted by publisher] for more detailed simulations about the model, which includes Ref. [14].
[24] B. Liu, L. Larsson, A. Caballero, X. Hao, D. Öling, J. Grantham, and T. Nyström, Cell **140**, 257 (2010).
[25] R. Spokoini, O. Moldavski, Y. Nahmias, J. L. England, M. Schuldiner, and D. Kaganovich, Cell Reports **2**, 738 (2012).
[26] C. Zhou, B. D. Slaughter, J. R. Unruh, F. Guo, Z. Yu, K. Mickey, A. Narkar, R. T. Ross, M. McClain, and R. Li, Cell **159**, 530 (2014).
[27] M. Coelho and I. M. Tolić, BioEssays **37**, 740 (2015).